

# **Phase transitions and critical phenomena of tiny grains thin films synthesized in microwave plasma chemical vapor deposition and origin of $\nu_1$ peak**

**Mubarak Ali,<sup>a,\*</sup> I-Nan Lin<sup>b</sup>**

<sup>a</sup> Department of Physics, COMSATS Institute of Information Technology, Islamabad 45550, Pakistan.

<sup>b</sup> Department of Physics, Tamkang University, Tamsui Dist., New Taipei City 25137, Taiwan (R.O.C.).

\*corresponding address: [mubarak74@comsats.edu.pk](mailto:mubarak74@comsats.edu.pk), [mubarak74@mail.com](mailto:mubarak74@mail.com) , Ph. +92-51-90495406

**Abstract-** Different trends have been observed in Raman analyses and electron field emission measurements of ultrananocrystalline diamond (UNCD) and nanocrystalline diamond (NCD) films synthesized in plasma-based chemical vapor deposition techniques. Phase transitions in any material are crucial as they may be the origin of new phenomenon. In the present work, it has been observed that dynamics determine the structure of tiny grains of UNCD and NCD films and those made in two-dimensional structure, they stretched in the direction of impinging electron streams of plasma. In those tiny grains where atoms stretch less photons of hard X-ray still retain their two-dimensional structure. On the other hand, those tiny grains where atoms are stretched more uniformly and suitably, on propagating photons through their electronic structures, they are transformed into grating like shapes. In Raman spectra, peaks related to  $\nu_1$  band and D\* band are due to those tiny grains of UNCD and NCD films which are transformed into grating like shapes and two-dimensional structures, respectively. Field emission characteristics of UNCD and NCD

films are resulted on the basis of tiny grains transformed into grating like shapes. High resolution transmission electron microscopy analyses physically show transforming of two different structures of tiny grains in so called UNCD and NCD films and validate the observations.

**Keywords:** Tiny grains; Dynamics; Phase transitions; Raman spectra; Field emission

### **Introduction:**

Development of materials in tiny size and probing their characteristics at nanoscale level requires a new sort of observations. Where dynamics influence the structure, phase transitions may be considered, thus, pronounced and different effects may result in those materials under critical phenomena. Large number of publications has appeared on fabrication of ultrananocrystalline diamond (UNCD) and nanocrystalline diamond (NCD) films under varying conditions and their synthesis methods mainly involve plasma-assisted chemical vapor deposition (CVD) techniques. Performances of these UNCD/NCD films are mainly addressed in terms of grains sizes, their distributions, binding energies of different phases and features of Raman peaks. In microwave plasma enhanced CVD (MPE-CVD), tiny grains of UNCD/NCD films are made through atom-to-atom amalgamation and the process dynamics may influence the atomic configurations. Such tiny grains are expected to heat locally, stretch *via* the impingement of electron streams and propagation of photons into their electronic structures during synthesis in microwave plasma chemical environment. In the published work on UNCD/NCD films reveals more or less stretching of tiny grains in HR-TEM images and it is hard to recognize most of the atoms in their spherical shapes. Principally, such tiny grains should reveal different phases depending on the dynamics of individual atoms and their localized heating. These provide strong incentive to investigate their structural transitions and critical phenomena.

In the present work, different UNCD/NCD films were synthesized in MPE-CVD system and their phase transitions were investigated. Structural relevance of tiny grains in terms of Raman spectra and field emission characteristics are studied in detail. Confusion has been going on since three decades regarding the origin of peak related to ' $\nu_1$  band' in Raman spectra and it was

considered to be due to the size of the grains or the presence of transpolyacetylene layers around tiny grains. Present study shows different phase transitions of tiny grains and indicates the real reason of peak related to ' $\nu_1$  band' along with critical phenomena of structures under which localized surface plasmons is disregarded.

### **Experimental details:**

To synthesize so called UNCD/NCD films, microwave plasma enhanced chemical vapor deposition (MPE-CVD) system (IPLAS-Cyrannus, 2.45 GHz) was utilized. A schematic of the MPE-CVD set up have been shown in previously published work [1]. N-type Si wafers (resistivity: 1-5 Ohm-cm) were used as substrate material. Nucleation duration was set to 30 minutes in each experiment, whereas, deposition time was 60 minutes. Prior to loading the samples in the chamber, substrates were cleaned by ultrasonic agitation for the duration of 30 minutes in methanol solution containing nanodiamond powders of 30 nm and titanium powders of 325 mesh to generate nucleation sites. The total mass flow rate was 200 sccm and was kept constant in each experiment. The substrate temperature was measured by K-type thermocouple and was  $700^{\circ}\text{C}\pm 10^{\circ}\text{C}$  in UNCD/NCD films synthesized with 6 %  $\text{H}_2$  in argon -rich methane mixture, whereas, the temperature was significantly lowered to  $500^{\circ}\text{C}\pm 10^{\circ}\text{C}$  in UNCD/NCD films which were synthesized without  $\text{H}_2$ . On increasing chamber pressure from 100 torr to 200 torr at constant microwave power (1400 watts) no remarkable difference in temperature was noted. Due to lower thermal conductivity of Ar than  $\text{H}_2$ , heating of substrate by plasma is greatly reduced in Ar-rich  $\text{CH}_4$  mixture [2]. Surface morphologies of various UNCD/NCD films were analyzed by Field Emission Scanning Electron Microscope (FE-SEM, ZEISS, Model: SIGMA). Peaks related to various phases were analyzed by Raman spectroscopy (Renishaw; 325 nm and HR800 UV; 632.8 nm). Electron field emission (EFE) measurements of UNCD/NCD films were made by using a tunable parallel plate set-up and  $I - V$  characteristics were measured by an electrometer (Keithley 237) under vacuum level of  $10^{-6}$  torr. Dark field, bright field, high resolution images and SAED patterns of various UNCD/NCD films were taken by HR-TEM (JEOL JEM2100F) operated at 200 kV. Photon energy of different bands

in UNCD/NCD films were deduced by core loss and low loss EELS. Plasma species formed in microwave chamber were detected *in-situ* by Optical Electron Spectroscopy (B&WTEK BTC 112E) in the range of 200 – 1050 nm.

### **Results and discussion:**

Surface morphologies of so called UNCD/NCD films synthesized at various chamber pressures are shown in Figures S1 (a) to S1 (c); at 150 torr more tiny grains are in needle-like shapes. In UNCD/NCD films synthesized at 100 torr and 200 torr, more tiny grains are in spherical-like shapes. Morphological features of tiny grains in film synthesized without H<sub>2</sub> gas (Figure S2) are almost similar to the morphological features of tiny grains in film synthesized at 6 % H<sub>2</sub> (Figure S1b). Raman spectra of different films synthesized at 100 torr, 150 torr and 200 torr are shown in Figure 1 (a) indicating different intensity levels of peaks related to 'ν<sub>1</sub> band'. The 'ν<sub>1</sub> band' is more pronounced in films synthesized at 100 torr and 200 torr compared to the film synthesized at 150 torr. On the other hand, the 'ν<sub>1</sub> band' is intensive in film synthesized without H<sub>2</sub> gas (Figure S3) compared to the films synthesized at 6% H<sub>2</sub> (Figure 1a). Field emission current density as a function of applied field at various chamber pressures is shown in Figure 1 (b). Film synthesized at 100 torr shows superior EFE properties where 'turn on field' is 11.52 V/μm (the lowest value) and the large EFE current density (> 2.0 mA/cm<sup>2</sup>). The 'turn on field' is the highest (25 V/μm) in the film synthesized at 150 torr, whereas, it is recorded 16.4 V/μm at 200 torr. Field emission current density as a function of applied field in different UNCD/NCD films synthesized without H<sub>2</sub> and with H<sub>2</sub> (3% and 6%) in Ar-rich CH<sub>4</sub> mixture are shown in Figures S4 (a-c). In Figures S4 (a) to S4 (c), the general trend of the 'turn on field' is more morphology-dependent; the value of 'turn on field' at 100 torr is lower than that at 150 torr (same trend is noted in Figure 1b). Under lower chamber pressure (at 100 torr), impingement of electron streams to tiny grains are highly effective and they are stretched uniformly, whereas, the large value of 'turn on field' in film synthesized at 200 torr (Figure S4a) was due to less stretching of tiny grains as the impinging electron streams are

less effective at higher chamber pressure (200 torr) and detailed discussions of those phenomena will be given in the following sections.

Dark field TEM images of UNCD/NCD film synthesized at 100 torr and 200 torr are shown in Figures S5 (a) and S6 (a) where smaller dark spots are related to isolated tiny grains and bigger dark spots are related to coalesced tiny grains and their contrast is more visible in bright field TEM images (Figures S5b and S6b); in some regions of the film tiny grains amalgamated and in some regions dispersed. SAED patterns of the same regions of films are shown in Figures S5 (c) and S6 (c) where intensity spots do not show precise rings related to various planes of diamond structure.

HR-TEM image taken from the UNCD/NCD film synthesized at 100 torr is shown in Figure 2 (c) and from the figure two regions of magnified images are shown in Figures 2 (a) and 2 (b). In Figure 2 (a), several tiny grains in two-dimensional structures are transformed into grating like shapes and are overlaid as well. However, Figure 2 (b) shows only one tiny grain transformed into grating like shape. The insert in Figure 2 (c) shows spectral analysis of the structure shown in Figure 2 (b), which also reveals grating like shape of the tiny grain. Figure S7 shows HR-TEM image taken from another region of UNCD/NCD film and highlights different features of the tiny grains transformed into grating like shapes (important portions are labelled). Gap between two grating like shapes labeled by (2) indicates formation of canal like channel which is referred as 'graphitic filament' [1, 3]. HR-TEM image taken from the UNCD/NCD film synthesized at 200 torr is shown in Figure 3 (c) and from the figure two regions of magnified images are shown in Figures 3 (a) and 3 (b), respectively. In Figure 3 (a), impinging electron streams for shorter period result into less stretching of tiny grain and photons emitted by the action of charged particles (of plasma) still retain electronic structure in two-dimensional structure; electronic shell (s) of atom is (are) approached to overlap into the next adjacent ones of one-dimensional arrays. In Figure 3 (b), tiny grains are stretched more and on propagating photons of hard X-rays their electronic structures are transformed into grating like shapes. A canal-like channel is formed between two gratings and is denoted by red dotted line in Figure 3 (b). The insert in Figure 3 (c) shows spectral analysis of less

stretched tiny grain of region 'a' and presents the features of nearly two-dimensional structure where intensity spots do not reveal the configuration as in the case of grating like shape (in the insert of Figure 2c).

Here, 'electronic structure' is referred to that structure where electronic shells of atoms of tiny grains stretched more or less under the influence of impinging electron streams and while their localized heating. Under more stretching of tiny grains having two-dimensional structures their electronic structures are transformed into smooth elements. Inter-spacing of such elements is referred to as 'working fields'. Elements and working fields in each grating like shape move parallel to each other and they possess equal widths ( $\sim 0.10 \text{ nm} = 1 \text{ \AA}$ ) as labeled in Figures 2 (b) and 3 (b). X-ray with photon of wavelength  $0.1 \text{ nm}$  is called hard X-ray and has energy  $10 \text{ keV}$  [4]. In fact, the lattice doesn't collectively oscillate on trapping/coupling of electromagnetic radiations and photons only flatten the electronic structure of lattice into smooth elements by transferring energy where one-dimensionally stretched electronic shells of atoms align along their cores under their localized heating. Where electron streams impinged normal to atoms of tiny grains, atoms do not stretch one-dimensionally and they reveal swelling and photons do not transform such structures of tiny grains into smooth elements. By varying the time of impinging electron streams and due to greater number of electronic shells in metallic elements we can alter the widths of elements and their inter-spacing distances in tiny metallic colloids (and their extended shapes) and we extensively studied the phenomenon in gold and silver (we will discuss somewhere else).

Core loss EELS of UNCD/NCD films at the same regions from where HR-TEM images were collected are shown in Figures S8 (a) and (b). In Figures S8 (a) and (b) regions of both the films synthesized at 100 torr and 200 torr show an abrupt rise near  $292 \text{ eV}$  ( $\sigma^*$ -band) and a large dip in the vicinity of  $305 \text{ eV}$ , which is referred to as the nature of diamond [5, 6]. In Figures S8 (a) and (b), both spectra show hump-like peaks at  $328 \text{ eV}$ . However, due to transformation of more tiny grains into grating like shapes, the peak is more pronounced in film synthesized at 100 torr. In low loss EELS, graphitic phase shows a prominent peak at  $s_3$  ( $27 \text{ eV}$ ), whereas, the a-C phase shows a

peak at  $s_1$  (22 eV) [6, 7], however, in Figure S9 (a) the peak at 27 eV is not present in film synthesized at 100 torr and it is not exactly at 22 eV in film synthesized at 200 torr [Figure S9 (b)], which indicate different rate of stretching of tiny grains in two different UNCD/NCD films. In Figure S9 (a), hump-like peak with maximum height at 65 eV is an indication of greater number of tiny grains, which are stretched more and their electronic structures are transformed into grating like shapes and this is in accordance to EFE measurement and HR-TEM investigations.

In Raman spectroscopy of UNCD/NCD films, the peak at  $1150\text{ cm}^{-1}$  has been attributed to nanocrystalline diamond [7-9], however, the  $\nu_1$  peak (at  $1150\text{ cm}^{-1}$ ) cannot originate from a nanodiamond or related  $sp^3$ -bonded phase but assigned to transpolyacetylene segments at grain boundaries and surfaces [10]. Nemanich *et al.* [8, 9] proposed that  $1150\text{ cm}^{-1}$  peak arises from nanocrystalline or amorphous diamond. In the Raman spectroscopy of UNCD/NCD film, the sharp peak at  $1332.1\text{ cm}^{-1}$  is the characteristic of diamond and broadening of the peak is related to the NCD grains [11]. In UNCD/NCD films, the peak at  $1150\text{ cm}^{-1}$  appears hypothetically due to CH bonds and is always linked to another peak at  $1450\text{ cm}^{-1}$ , and the peaks at  $1330\text{ cm}^{-1}$  and  $1560\text{ cm}^{-1}$  are due to D- band and G-band [12]. However, in the light of presented results of UNCD films, argon gas increases the rate of re-nucleation and the amount of tiny grains sizes  $< 10\text{ nm}$  is enhanced significantly, also in NCD film more tiny grains have size  $> 10\text{ nm}$  and depending on how many tiny grains are transformed structures into grating like shapes experienced excitations on exposure to Raman laser, from this the contributions are in the form of peak and appear at wave number  $1150\text{ cm}^{-1}$ . In microcrystalline diamond films, the size of grain is very large and atoms are more in tetrahedron structure, accordingly, information put forth by Raman spectrum doesn't show any peak at  $1150\text{ cm}^{-1}$ . Thus, the peak in UNCD/NCD films at wave number  $1150\text{ cm}^{-1}$  is associated to those tiny grains transformed into grating like shapes and depending on their quantity excitations levels are altered followed by the variation in the intensity of ' $\nu_1$  peak'; different intensities of ' $\nu_1$  band' are related to the number of the tiny grains transformed into grating like shapes. Now, those tiny grains, which are transformed into grating like shapes, electronic

excitations are executed at higher energy comparatively to both tetrahedron and disordered structures of the film, thus, ' $\nu_1$  peak' is originated at wave number  $1150\text{ cm}^{-1}$ . Prior to transforming tiny grains into grating like shape, they were in two-dimensional structure and according to fundamental of materials science, the packing factor of such structure is greater than tetrahedron structure. Obviously, the peak at wave number  $\sim 1150\text{ cm}^{-1}$  is linked to greater packing factor of the grating like structure. Due to lower packing factor of the diamond structure, the peak is recorded at wave number  $1332\text{ cm}^{-1}$ . Briefly, on exposure of Raman laser to the film, Raman signals recorded intensities depending on the energy of phase, thus, peaks are originated at different wave numbers, that is, more the energy of phase less is the wavelength of peak (and higher is the wave number). In the Raman spectrum, the positions of peaks of different carbon phases is in accordance to the Planks' equation of energy –wavelength. Thus, we conclude that ' $\nu_1$  band' is not due to size of tiny grain itself or layer of transpolyacetylene present around them but is related to electronic excitations in the tiny grains, which are transformed into grating like shapes. Incorporating  $\text{H}_2$  in Ar-rich  $\text{CH}_4$  mixture either eliminates the ' $\nu_1$  band' or it appears with less intensity. Without addition of  $\text{H}_2$  in Ar-rich  $\text{CH}_4$  mixture, peak related to ' $\nu_1$  band' becomes pronounced (Figure S3). On varying concentrations of gases, the nature of tiny grains both in terms of physics and chemistry is altered and UNCD/NCD films count different numbers of tiny grains, which are transformed into grating like shapes and this turns into different intensities of ' $\nu_1$  band'; on penetrating different wavelengths of Raman signals in UNCD/NCD films different intensities of ' $\nu_1$  band' are discernable [13, 14]. Optical Emission Spectra taken at various chamber pressures is in accordance to Raman spectroscopy of UNCD/NCD films (Figure S10) where peak related to  $\text{H}_2$  gas was absent in the film synthesized without  $\text{H}_2$  gas and indicates the stabilization of plasma through atomic hydrogen, which was resulted on disassociating  $\text{CH}_4$ . Optical Emission Spectra (OES) taken at various chamber pressures are shown in Figure S10 where the same trend of emission intensities of CH and C2 was observed. OES collected for 10 seconds in each experiment with regular intervals and revealed the same results in terms of emission intensities of CH and C2 (Figure S10). For films

synthesized without hydrogen, hydrogen species are not present in OES and there was very little amount of hydrogen involved in the process of C-H formation (during the growth of UNCD/NCD films) and support the results of Raman spectroscopy. At zero % H<sub>2</sub>, the source of small amount of hydrogen was the CH<sub>4</sub>, which dissociate in microwave chamber as the result of microwave power. Collisions of energetic argon species facilitate the dissociation of CH<sub>4</sub> [15]. As shown in Figure S10, the nature of plasma changed in the chemical reactor; up to 20 torr pressure, high intensity peaks of Ar-I are present. As the chamber pressure exceed, high intensity peaks of C2 radicals is appeared while Ar peaks is disappeared and plasma is fully ionized. An earlier in-situ OES study of Ar-rich microwave plasma shows similar type of Ar emission over wavelength 700 nm [16]. In the absence of H<sub>2</sub> gas, it is believed that some hydrogen atoms come from the disassociation of CH<sub>4</sub> and assist plasma to be stabilized [17]. As a result of microwave power, argon atoms are excited and dissociate CH<sub>4</sub> molecules for their activation [15]. OES of processing plasma in microwave plasma chamber have been worked out by number of groups [18, 19], which show similar type of information as shown in Figure S10.

Impinging electron streams stretched atoms of tiny grains having two-dimensional structures in the direction of their impingement, as consequence of this, electronic shells of atoms overlapped into the next adjacent ones of each one-dimensional array. In due course of time, photons emitted through the interactions of charged particles, their propagation into one-dimensionally stretched electronic shells of atoms flatten them into smooth elements by utilizing their energy. Briefly, under the regime of dynamics those tiny grains configured two-dimensional structure they stretched uniformly in the direction of impingement of electron streams and on propagating photons they either transformed their electronic structures into two-dimensional lattices (those stretched less) or into grating like shapes (those stretched more). In out of equilibrium system, different interactions contributed to induce electronic/ionic temperatures [20]. Ye *et al.* [21] predicted the local temperature of a system out of equilibrium. A schematic presentation of tiny grain where atoms are configured into two-dimensional structure (25 atoms) under dynamics is shown in Figure 4 (a).

Impinging electron streams for less or more time stretched tiny grain in the direction of their impingement; less stretched electronic structure of tiny grain is shown in Figure 4 (b) while more stretched electronic structure of tiny grain is shown in Figure 4 (c). In less stretched electronic structure of tiny grain photons retained the structure two-dimensional (Figure 4d), whereas, in more stretched tiny grain photons transformed electronic structure into smooth elements (Figure 4e).

### **Conclusions:**

In microwave plasma chemical vapour deposition environment, discernible phase transitions of two dominant structures of tiny grains in UNCD/NCD films have been observed. A tiny grain in two-dimensional structure is made through atom-to-atom amalgamation under the process dynamics while localized heating. Such tiny grains stretch more or less in the direction of impingement of electron streams depending on the time of impinging electron streams and those stretched less propagating photons at air (plasma)-semi-metal interface still retain their two-dimensional structure, whereas, those tiny grains stretched more propagating photons through their electronic structures transform them into grating like shapes in which electronic shells of atoms overlapped into the next adjacent ones of one-dimensional arrays. This process of overlapping of electronic shells of atoms into the next adjacent ones of one-dimensionally stretched arrays in the direction of impingement and propagating photons through their electronic structures disregard the phenomenon of localized surface plasmons. In Raman spectrum, tiny grains in grating like shapes are the origin of ' $\nu_1$  peak', whereas, those tiny grains still retaining their two-dimensional structures are the origin of  $D^*$  peak. Phase transitions of tiny grains are critical phenomena in determining the overall performance of various UNCD/NCD films and play crucial role in evaluating the performance of films for various applications. The lower 'turn on field' of UNCD/NCD film is due to transformation of more tiny grains into grating like shapes. HR-TEM images of tiny grains in UNCD/NCD films reveal different mechanisms of their transformation; in some regions they assemble tip-to-tip and extend in size, in some regions their assembling display different orientations, in other regions they leave very small distance between each other and non-regular surfaces appear (so called 'grain

boundaries'), while in some regions there are broad distances and leave wide gaps, in some regions overlay and coalesce with non-uniform stretching of their atoms. In fact, all those phenomena contribute into the measurement of the performance of UNCD/NCD films and the most influential factor is related to those tiny grains transformed into grating like shapes. Thus, characteristics of different UNCD/NCD films in term of electron field emission are not merely due to electron affinity, thermal behavior of phases, doping and charge transfer. In line with this, present studies set a new horizon in synthesizing, analyzing and evaluating the materials at nanoscale, and solicit reinvestigation of materials' performances both in existing and future applications.

#### **Acknowledgements:**

Mubarak Ali thanks National Science Council (now MOST) Taiwan (R.O.C.) for awarding postdoctorship: NSC-102-2811-M-032-008 (2013-2014). Authors wish to thank Mr. Tsung-Min Chen for assisting films' synthesis and Mr. Chien-Jui Yeh in TEM operation. Mubarak Ali greatly appreciates useful suggestions of Dr. M. Ashraf Atta and Dr. Abdul Waheed (CIIT, advisors).

#### **References:**

- [1] A. Saravanan, B. R. Huang, K. J. Sankaran, G. Keiser, J. Kurian, N. H. Tai, I. N. Lin, Structural modification of nanocrystalline diamond films via positive/negative bias enhanced nucleation and growth processes for improving their electron field emission properties, *J. Appl. Phys.* 117 (2015) 215307-11.
- [2] X. Xiao, J. Birrell, J. E. Gerbi, O. Auciello, J. A. Carlisle, Low temperature growth of ultrananocrystalline diamond, *J. Appl. Phys.* 96 (2004) 2232-2239.
- [3] S. C. Lin, C. -J. Yeh, C. L. Dong, H. Niu, J. Kurian, K. -C. Leou, I -N. Lin, The microstructural evolution of ultrananocrystalline diamond films due to P ion implantation and annealing process-dosage effect, *Diam. Relat. Mater.* 54 (2015) 47-54.
- [4] D. Attwood, *Soft X-rays and extreme ultraviolet radiation (Principles and Applications)*. Cambridge University Press, pp. 1-2 (1999).

- [5] D. M. Gruen, S. Liu, A. R. Krauss, X. Pan, Buckyball microwave plasmas: Fragmentation and diamond-film growth, *J. Appl. Phys.* 75 (1994) 1758-1763.
- [6] P. Kovarik, E. B. D. Bourdon, R. H. Prince, Electron-energy-loss characterization of laser-deposited *a*-C, *a*-C:H, and diamond films, *Phys. Rev. B* 48 (1993) 12123-12129.
- [7] W. A. Yarbrough, R. Messier, Current issues and problems in the chemical vapor deposition of diamond, *Science* 247 (1990) 688-696.
- [8] R. J. Nemanich, J. T. Glass, G. Lucovsky, R. E. Shroder, Raman scattering characterization of carbon bonding in diamond and diamondlike thin films, *J. Vac. Sci. Technol. A* 6 (1988) 1783-1787.
- [9] R. E. Shroder, R. J. Nemanich, J. T. Glass, Analysis of the composite structures in diamond thin films by Raman spectroscopy, *Phys. Rev. B* 41 (1990) 3738-3745.
- [10] A. C. Ferrari, J. Robertson, Origin of the  $1150\text{cm}^{-1}$  Raman mode in nanocrystalline diamond, *Phys. Rev. B* 63 (2001) 121405-5.
- [11] I. Jiménez, M. M. García, J. M. Albella, L. J. Terminello, Orientation of graphitic planes during the bias-enhanced nucleation of diamond on silicon: An x-ray absorption near-edge study, *Appl. Phys. Lett.* 73 (1998) 2911-2913.
- [12] J. Birrell, J. E. Gerbi, O. Auciello, J. M. Gibson, J. Johnson, J. A. Carlisle, Interpretation of the Raman spectra of ultrananocrystalline diamond, *Diam. Relat. Mater.* 14 (2005) 86-92.
- [13] R. Haubner, M. Rudigier, Raman characterisation of diamond coatings using different laser wavelengths, *Physics Procedia* 46 (2013) 71-78.
- [14] S. C. Ray, I -N. Lin, Ferroelectric behaviours of ultra-nano-crystalline diamond thin films, *Surf. Coat. Technol.* 271 (2015) 247-250.
- [15] S. J. Askari, F. Lu, Characteristics of a well-adherent nanocrystalline diamond thin film grown on titanium in Ar/CH<sub>4</sub> microwave CVD plasma, *Vacuum* 82 (2008) 673-677.
- [16] C. -R. Lin, *et al.*, Fabrication of highly transparent ultrananocrystalline diamond films from focused microwave plasma jets, *Surf. Coat. Technol.* 231 (2013) 594-598.

- [17] P. W. May, Y. A. Mankelevich, From Ultrananocrystalline Diamond to Single Crystal Diamond Growth in Hot Filament and Microwave Plasma-Enhanced CVD Reactors: a Unified Model for Growth Rates and Grain Sizes, *J. Phys. Chem. C* 112 (2008) 12432-12441.
- [18] Y. -C. Chu, et al., Systematic studies of the nucleation and growth of ultrananocrystalline diamond film on silicon substrates coated with a tungsten layer, *J. Appl. Phys.* 111 (2012) 124328-36.
- [19] J. -H. Jiang, Y. Tzeng, Mechanisms of suppressing secondary nucleation for low-power and low temperature microwave plasma self-bias-enhanced growth of diamond films in argon diluted methane, *AIP Advances* 1 (2011) 042117-11.
- [20] M. D. Ventra, *Electrical Transport in Nanoscale Systems* (Cambridge University Press, Cambridge, 2008).
- [21] L. Ye, D. Hou, X. Zheng, Y. Yan, M. D. Ventra, Local temperatures of strongly-correlated quantum dots out of equilibrium, *Phys. Rev. B* 91 (2015) 205106-8.

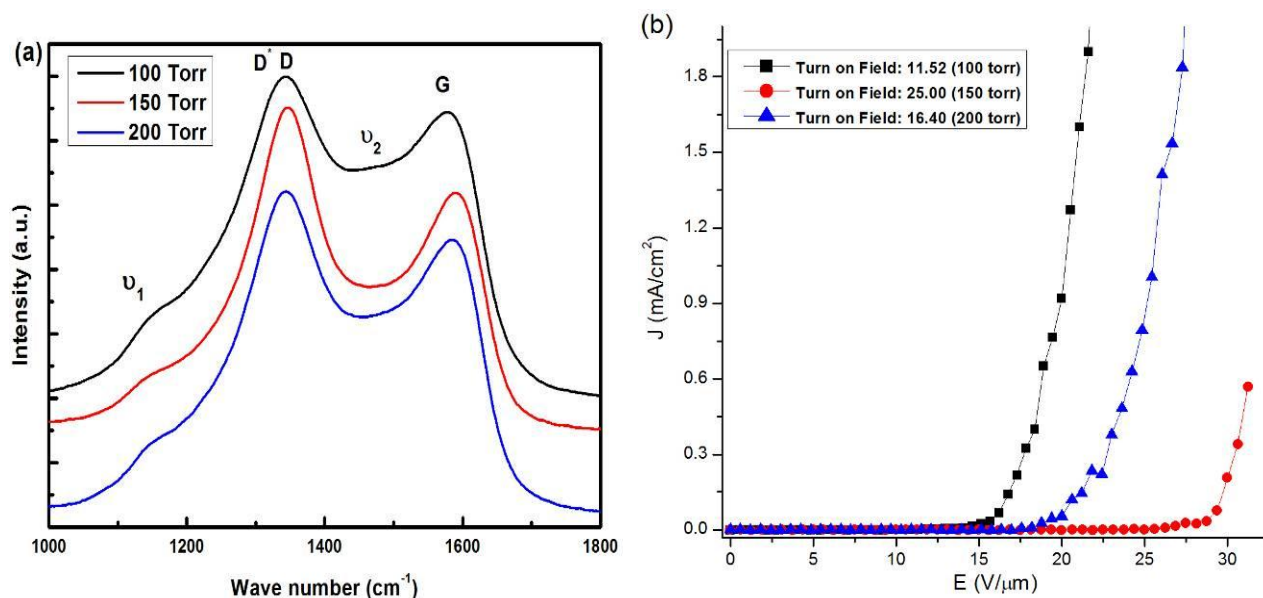


**Figure 1:** (a) Raman spectra and (b) electron field emission current density as a function of applied field of UNCD/NCD films synthesized at chamber pressure 100 torr, 150 torr and 200 torr; total mass flow rate: 200 sccm (6% H<sub>2</sub>, 1 % CH<sub>4</sub> and 93 % argon, Ar: CH<sub>4</sub>: H<sub>2</sub> = 186:2:12), microwave power: 1400 watts and deposition time: 60 minutes

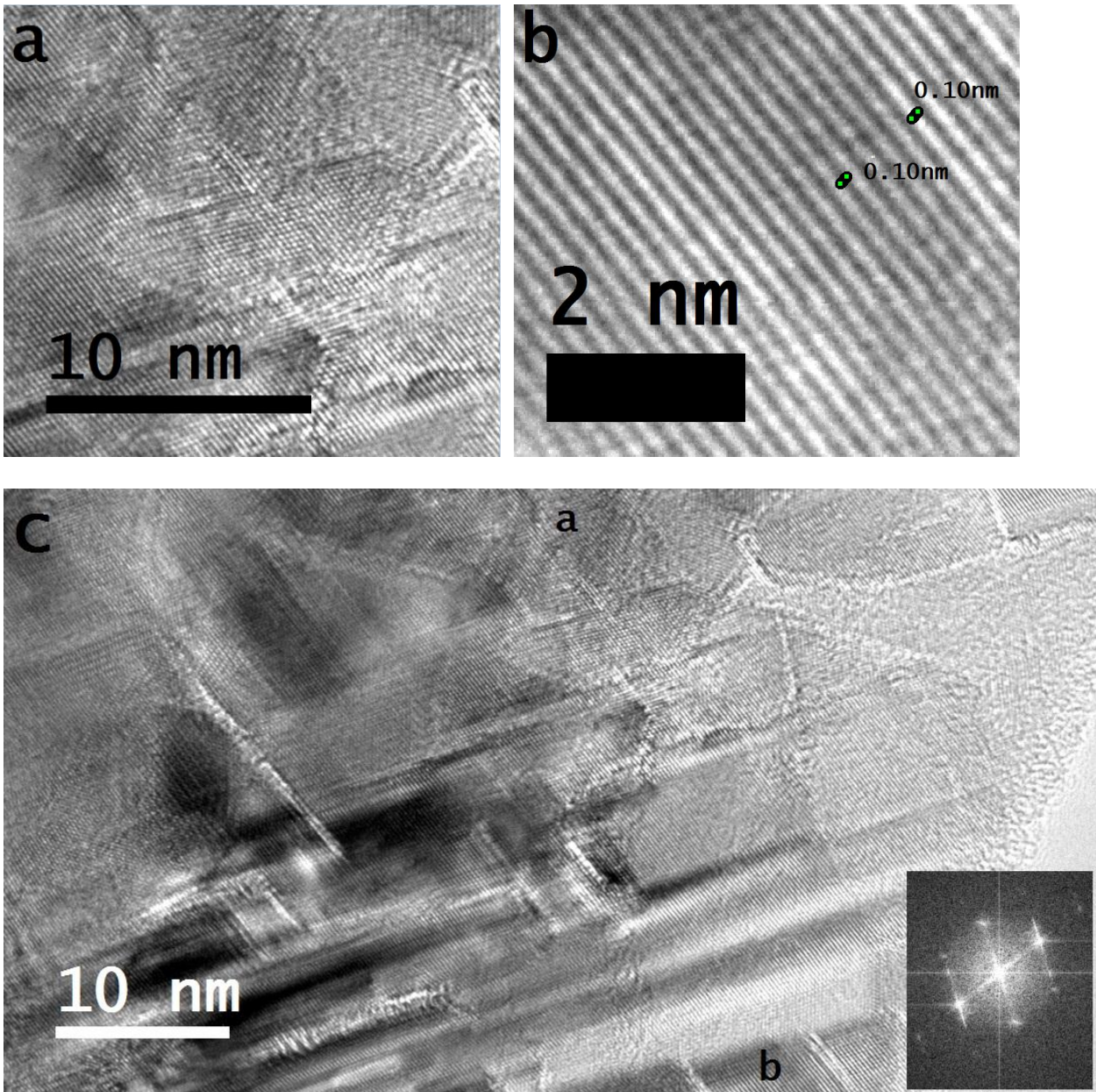


**Figure 2:** (a) Magnified region of HR-TEM image shows overlaying of grating like shapes, (b) magnified region of HR-TEM image shows grating like shape and (c) standard HR-TEM image shows large number of tiny grains transformed into grating like shapes; UNCD/NCD film synthesized at chamber pressure: 100 torr, mass flow rate: 200 sccm (6% H<sub>2</sub>, 1 % CH<sub>4</sub> and 93 % argon), microwave power: 1400 watts and deposition time: 60 minutes.

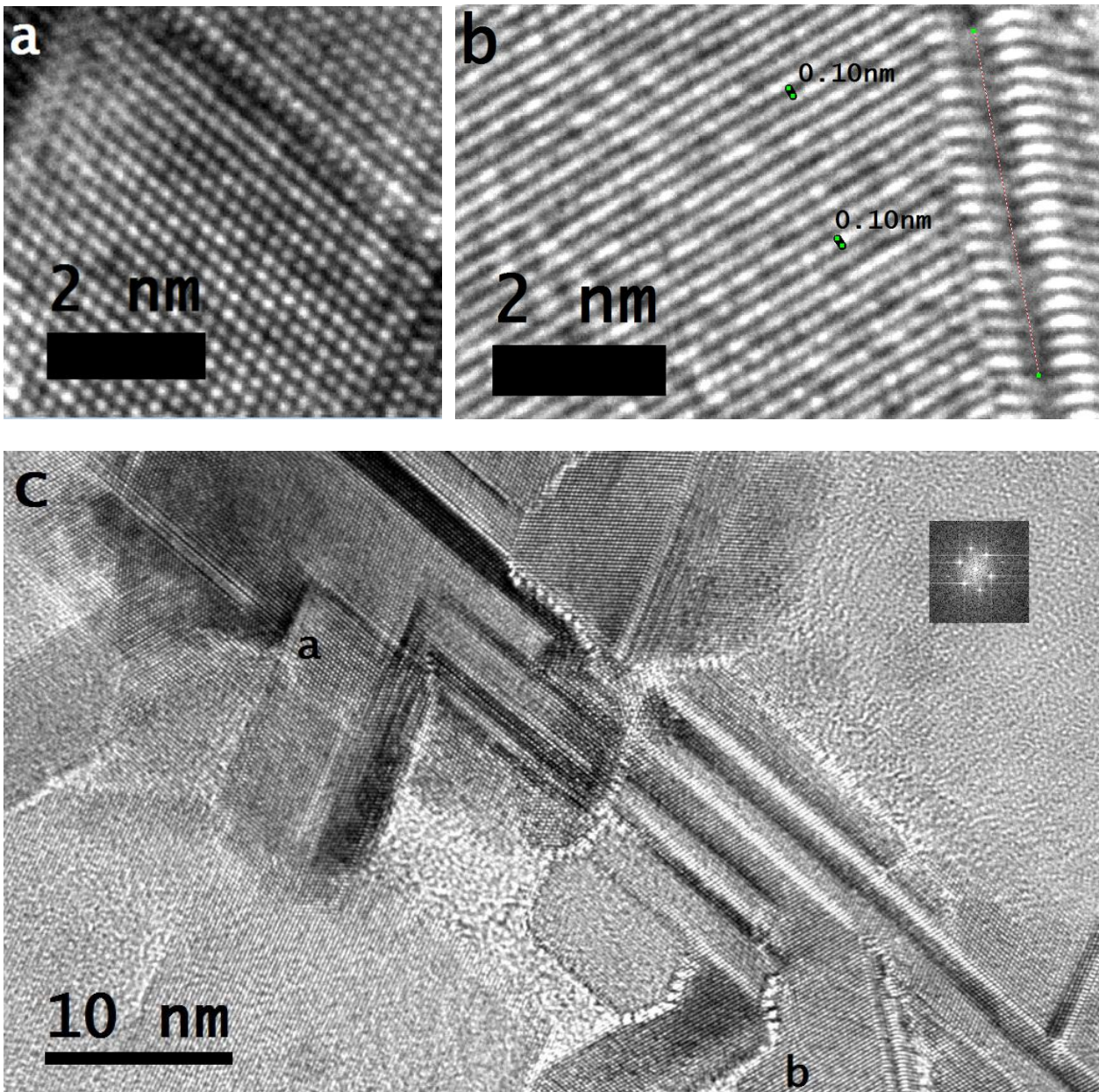


**Figure 3:** (a) Magnified region of HR-TEM image shows two-dimensional lattice, (b) magnified region of HR-TEM image shows grating like shape and (c) standard HR-TEM image shows several tiny grains retained two-dimensional structures and grating like shapes as well (insert shows spectral analysis of region 'a'); UNCD/NCD film synthesized at chamber pressure: 200 torr, mass flow rate: 200 sccm (6% H<sub>2</sub>, 1 % CH<sub>4</sub> and 93 % argon), microwave power: 1400 watts and deposition time: 60 minutes.

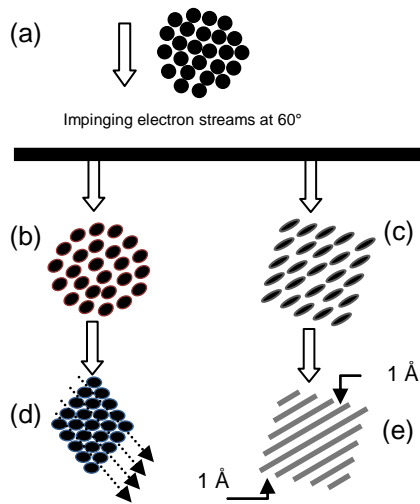


**Figure 4:** (a) Compact two-dimensional structure of tiny grain, (b) less stretching of tiny grain (c) more stretching of tiny grain, (d) transformation of electronic structure of less stretched tiny grain into two-dimensional lattice and (e) transformation of electronic structure of more stretched tiny grain into grating like shape.

## Supplementary Materials

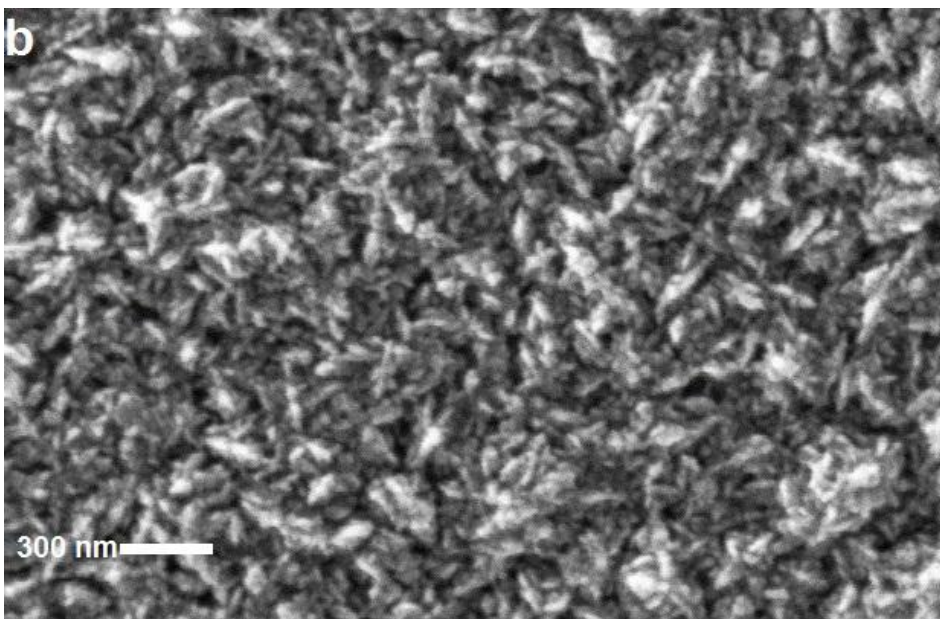
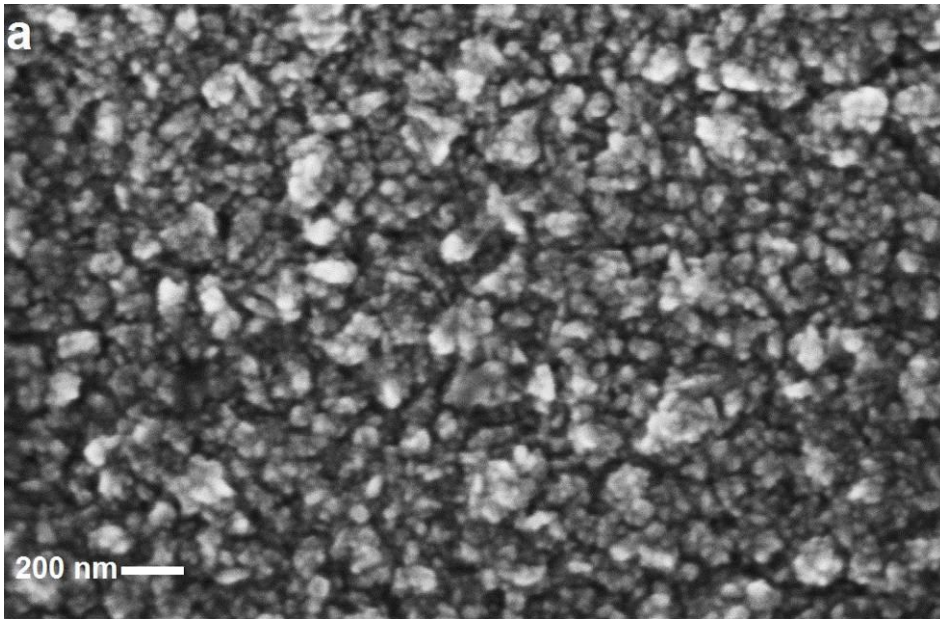
### **Phase transitions and critical phenomena of tiny grains thin films synthesized in microwave plasma chemical vapor deposition and origin of $\nu_1$ peak**

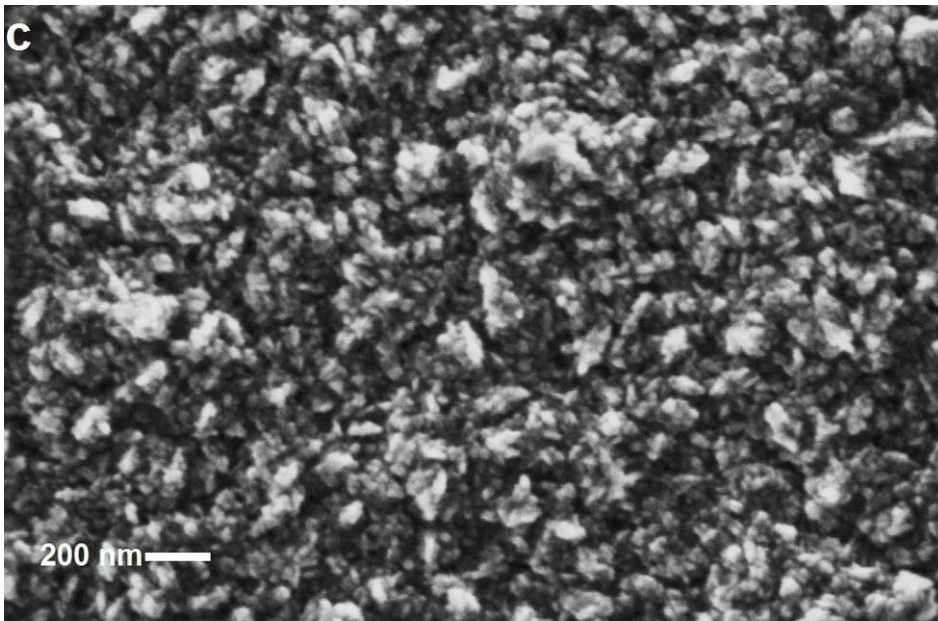
**Mubarak Ali,<sup>a,\*</sup> I-Nan Lin<sup>b</sup>**

<sup>a</sup> Department of Physics, COMSATS Institute of Information Technology, Islamabad 45550, Pakistan.

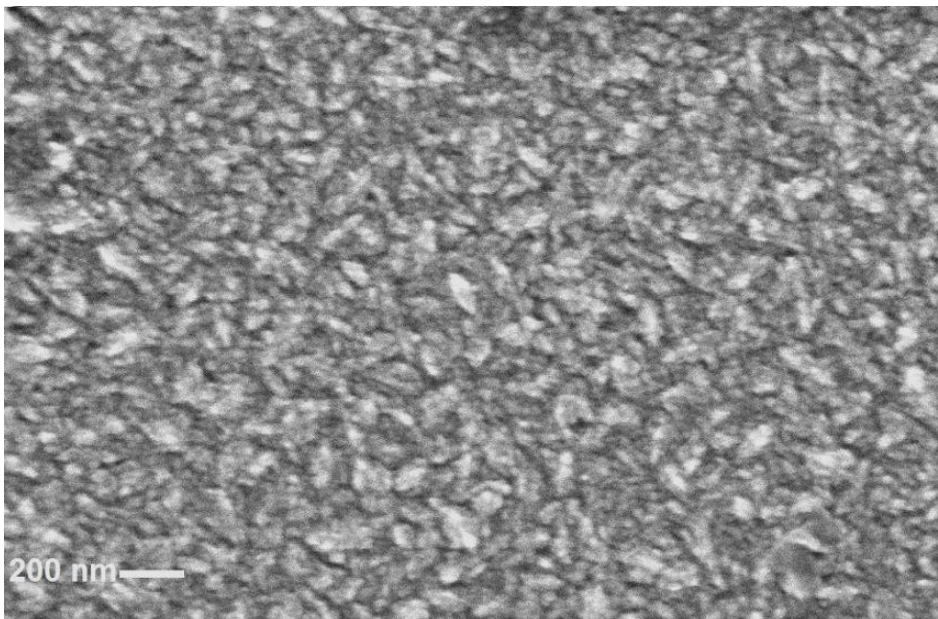
<sup>b</sup> Department of Physics, Tamkang University, Tamsui Dist., New Taipei City 25137, Taiwan (R.O.C.).

\*corresponding address: [mubarak74@comsats.edu.pk](mailto:mubarak74@comsats.edu.pk), [mubarak74@mail.com](mailto:mubarak74@mail.com) , Ph. +92-51-90495406

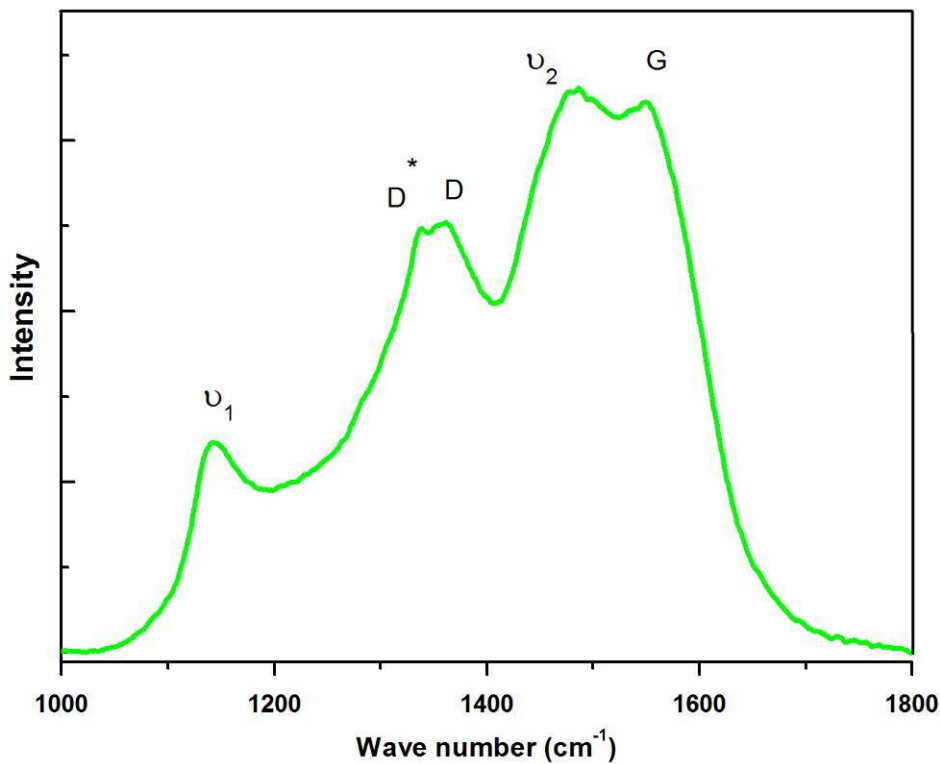




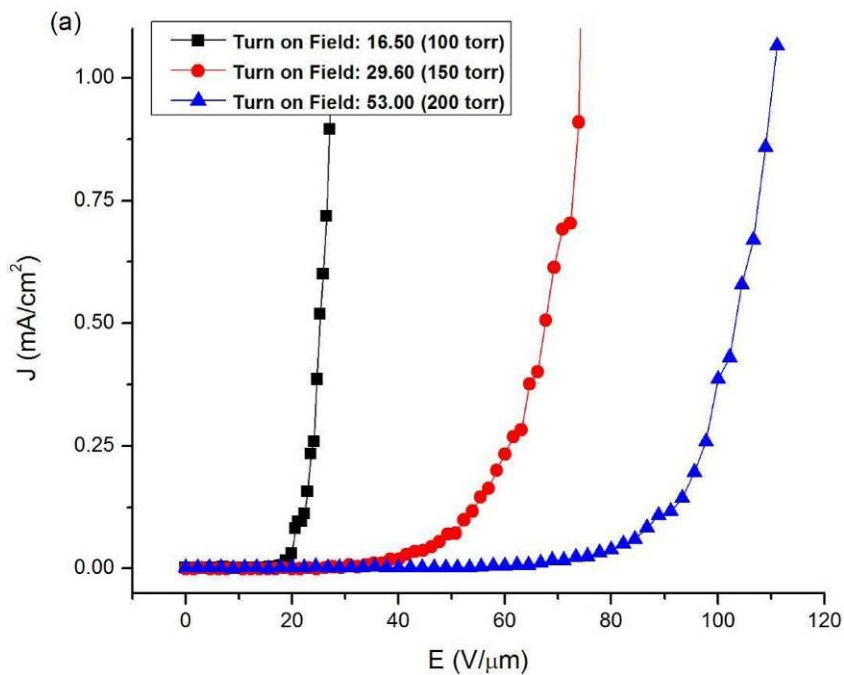
**Figure S1:** Surface morphologies of UNCD/NCD films synthesized at chamber pressure (a) 100 torr, (b) 150 torr, and (c) 200 torr; total mass flow rate: 200 sccm (6% H<sub>2</sub>, 1 % CH<sub>4</sub> and 93 % argon, Ar: CH<sub>4</sub>: H<sub>2</sub> = 186:2:12), microwave power: 1400 watts and deposition time: 60 minutes.

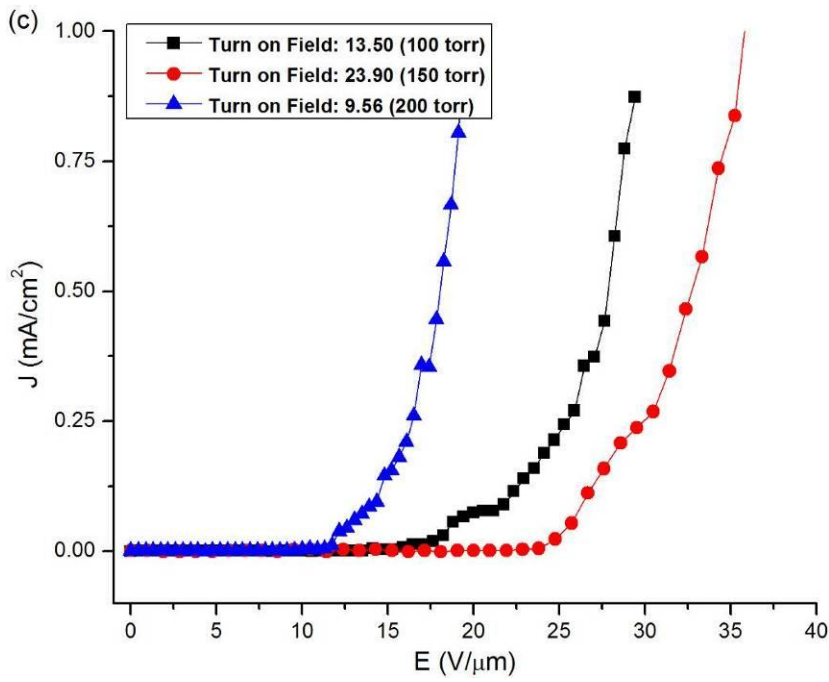
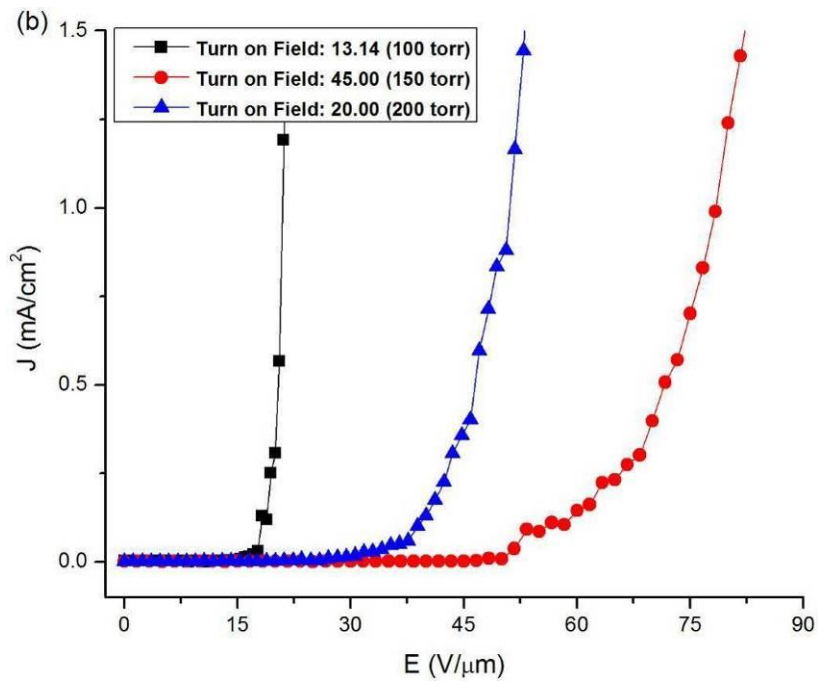


**Figure S2:** Surface morphology of UNCD/NCD film synthesized at chamber pressure 150 torr; total mass flow rate: 200 sccm (0% H<sub>2</sub>, 2 % CH<sub>4</sub> and 98 % argon, Ar: CH<sub>4</sub>: H<sub>2</sub> = 196:4:0), microwave power: 1100 watts and deposition time: 60 minutes.

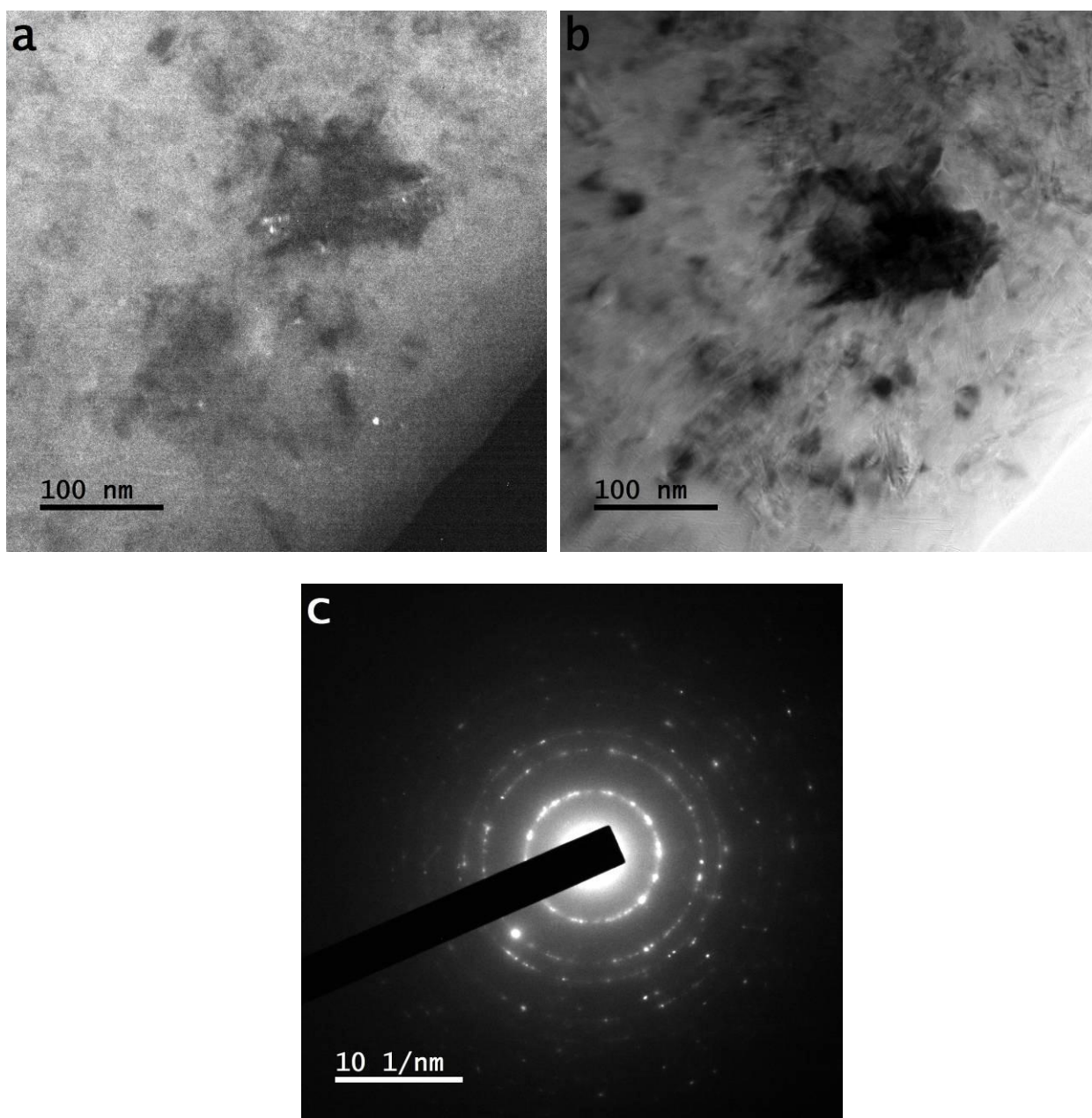


**Figure S3:** Raman spectrum of UNCD/NCD film synthesized at chamber pressure 150 torr; total mass flow rate: 200 sccm (0%  $\text{H}_2$ , 2 %  $\text{CH}_4$  and 98 % argon, Ar:  $\text{CH}_4$ :  $\text{H}_2$  = 196:4:0), microwave power: 1100 watts and deposition time: 60 minutes ( $\nu_1$ :  $\sim 1145 \text{ cm}^{-1}$ ,  $D^*$ :  $\sim 1310 \text{ cm}^{-1}$ ,  $D$ :  $1332 \text{ cm}^{-1}$ ,  $\nu_2$ :  $\sim 1480 \text{ cm}^{-1}$ ,  $G$ :  $\sim 1580 \text{ cm}^{-1}$ ).

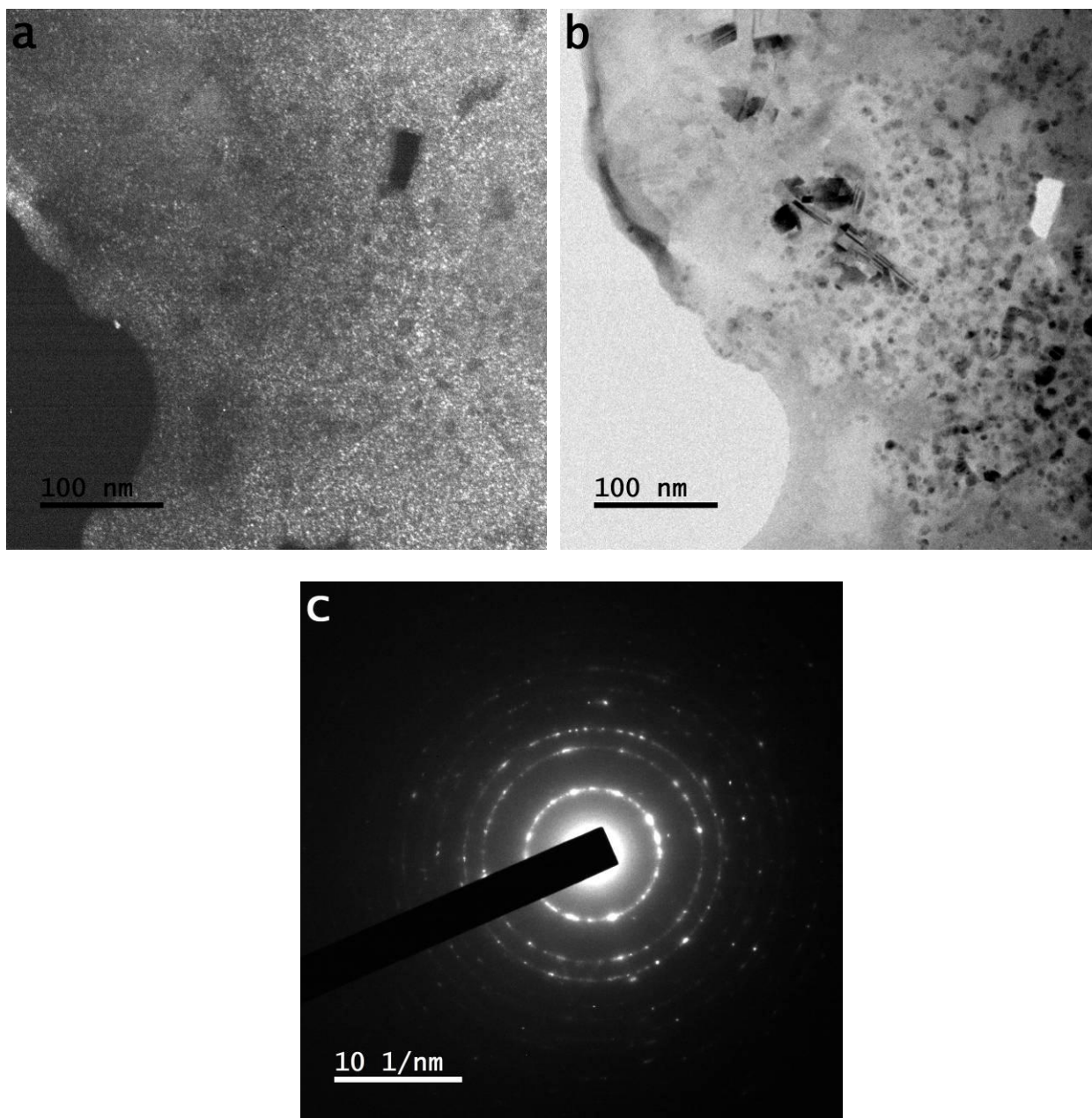




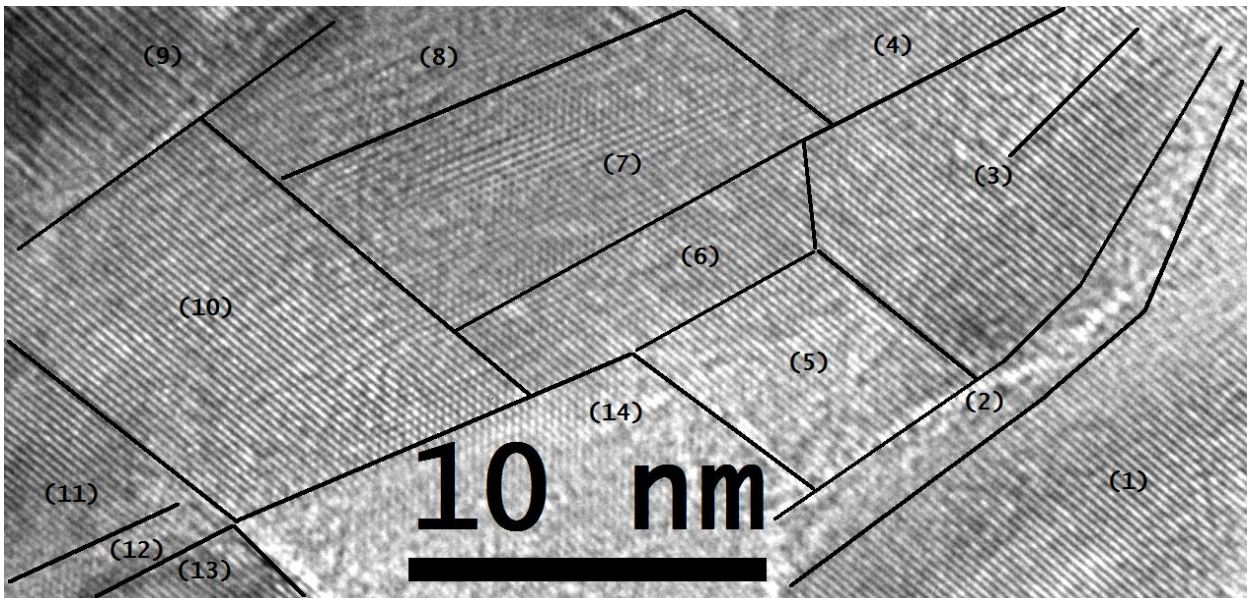
**Figure S4:** Electron field emission current density as a function of applied field of UNCD/NCD films synthesized at (a) without H<sub>2</sub>, (b) 3 % H<sub>2</sub> and (c) 6 % H<sub>2</sub>; 1 % CH<sub>4</sub>, total mass flow rate: 200 sccm, microwave power: 1200 watts and deposition time: 60 minutes.



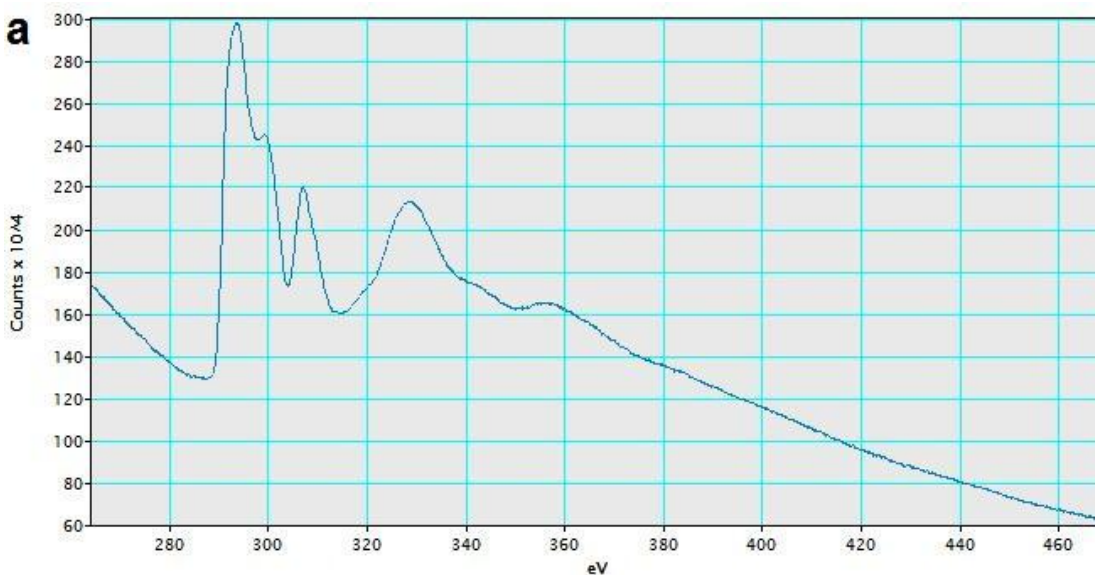
**Figure S5:** (a) Dark field TEM image (b) Bright field TEM image and (c) SAED pattern of UNCD/NCD film synthesized at chamber pressure: 100 torr, total mass flow rate: 200 sccm (6% H<sub>2</sub>, 1 % CH<sub>4</sub> and 93 % argon), microwave power: 1400 watts and deposition time: 60 minutes.

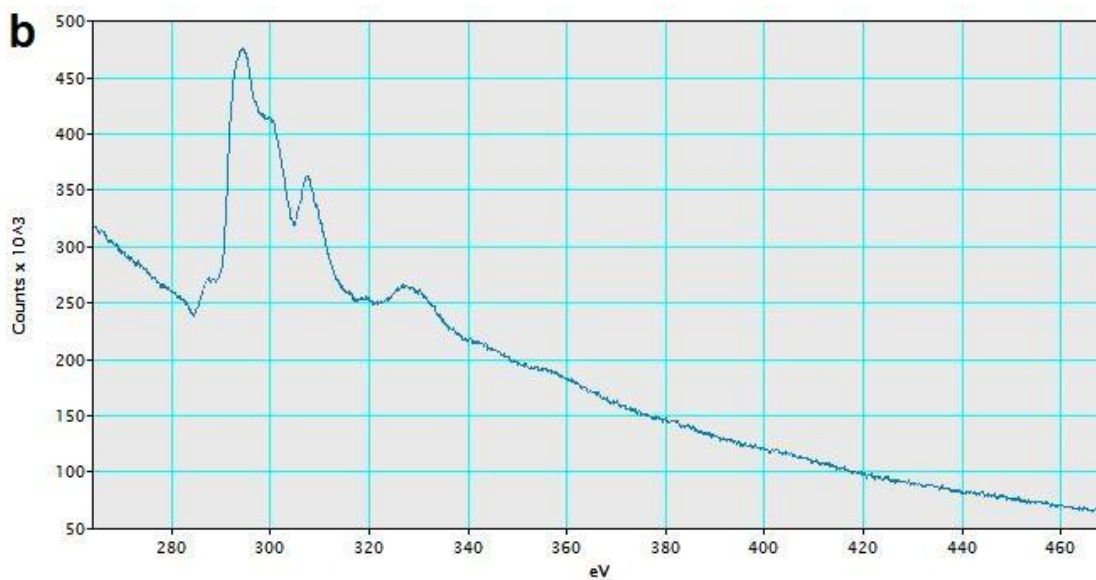


**Figure S6:** (a) Dark field TEM image (b) Bright field TEM image and (c) SAED pattern of UNCD/NCD film synthesized at chamber pressure: 200 torr, total mass flow rate: 200 sccm (6% H<sub>2</sub>, 1 % CH<sub>4</sub> and 93 % argon), microwave power: 1400 watts and deposition time: 60 minutes.

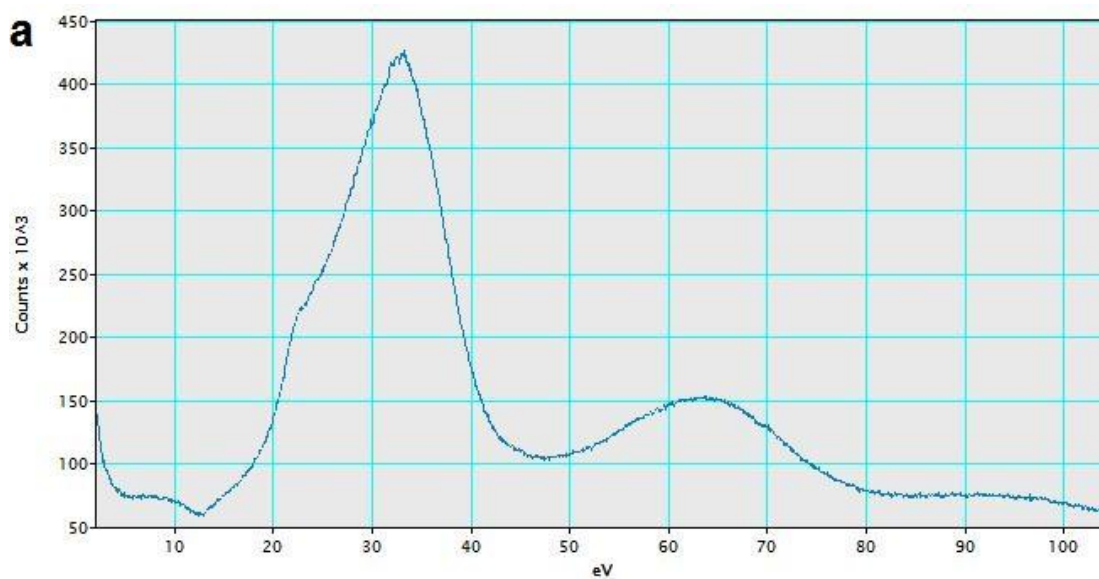


**Figure S7:** HR-TEM image of UNCD/NCD film synthesized at chamber pressure 100 torr shows differently transformed tiny grains; (1, 4, 6 and 10) grating like shapes, (2 and 12) canals between grating like shapes, (3) tip-to-tip assembling in two grating like shapes, (5, 7, 11 and 13) tiny grains partially transformed into grating like shapes and non-uniform stretching of lattices, (8 and 9) more atoms of tiny grains reveal swelling and in some cases do not form compact configurations and (14) unoccupied space covered the grating like shape; total mass flow rate: 200 sccm (6% H<sub>2</sub>, 1 % CH<sub>4</sub> and 93 % argon), microwave power: 1400 watts and deposition time: 60 minutes.





**Figure S8:** Core Loss EELS of UNCD/NCD films synthesized at chamber pressure (a) 100 torr and (b) 200 torr; total mass flow rate: 200 sccm (6% H<sub>2</sub>, 1 % CH<sub>4</sub> and 93 % argon), microwave power: 1400 watts and deposition time: 60 minutes.



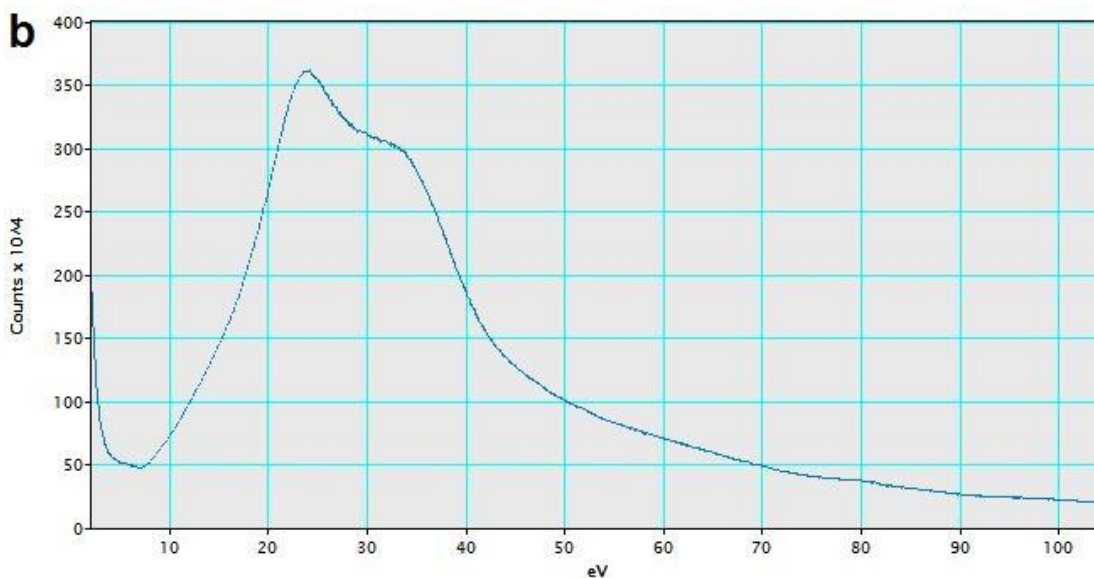


**Figure S9:** Low loss EELS of UNCD/NCD films synthesized at chamber pressure (a) 100 torr and (b) 200 torr; total mass flow rate: 200 sccm (6% H<sub>2</sub>, 1 % CH<sub>4</sub> and 93 % argon), microwave power: 1400 watts and deposition time: 60 minutes.

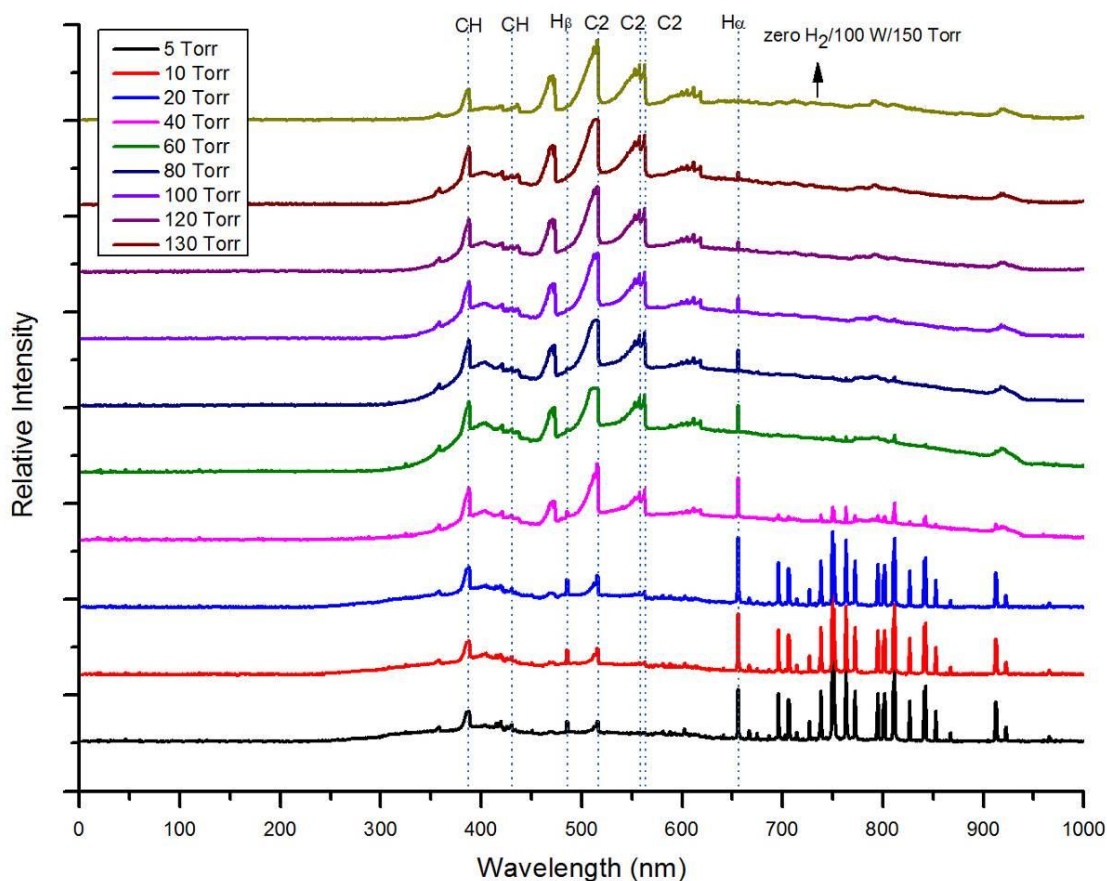


**Figure S10:** Optical Emission Spectra of the processing plasma at various chamber pressure at total mass flow rate: 200 sccm (3% H<sub>2</sub>, 1 % CH<sub>4</sub> and 96 % argon) and microwave power: 1300 watts.